# Image quality of cone beam CT on respiratory motion

ZHANG Ke[1] LI Minghui[1] DAI Jianrong[1,*] WANG Shi[2,*]

[1]*Department of Radiation Oncology*, *Cancer Institute* (*Hospital*), *Chinese Academy of Medical Sciences*, *Beijing 100021*, *China*

[2]*Department of Engineering Physics*, *Tsinghua University*, *Beijing 100084*, *China*

**Abstract** In this study, the influence of respiratory motion on Cone Beam CT (CBCT) image quality was investigated by a motion simulating platform, an image quality phantom, and a kV X-ray CBCT. A total of 21 motion states in the superior-inferior direction and the anterior-posterior direction, separately or together, was simulated by considering different respiration amplitudes, periods and hysteresis. The influence of motion on CBCT image quality was evaluated with the quality indexes of low contrast visibility, geometric accuracy, spatial resolution and uniformity of CT values. The results showed that the quality indexes were affected by the motion more prominently in AP direction than in SI direction, and the image quality was affected by the respiration amplitude more prominently than the respiration period and the hysteresis. The CBCT image quality and its characteristics influenced by the respiration motion, and may be exploited in finding solutions.

**Key words** Respiratory motion, Cone beam CT, Image quality

## 1 Introduction

The kV X-ray cone beam computer tomography (CBCT) can be used to correct patient setup error[1–3], and perform adaptive image-guided radiotherapy[4–6]. However, the CBCT image quality for the patient with thoracic or upper abdomen tumors is usually affected by respiration motion of anatomical structure, resulting in image blur or worse artifacts. The image registration and target definition is affected, too. Therefore, it is essential to investigate the influence of respiration motion on CBCT image quality. Ju-Young Song *et al.*[7] used a 1D motion apparatus, and the head and neck cube in an I'mRT Phantom designed for dosimetry quality assurance of IMRT to simulate respiratory motion. The impact of respiratory motion on the image quality was evaluated with the CT number variations along the center line of coronal images. In this work, we used a 2D motion simulating apparatus (Mapcheck XY/4D Table, Sun Nuclear, Melbourne, FL, USA) and a CT image quality phantom (CatPhan503, Phantom Laboratory, Salem, NY, USA). The observed image quality indexes were of low contrast visibility, geometric accuracy, spatial resolution (line pair and MTF), and uniformity of CT values.

## 2 Material and methods

### 2.1 Motion simulation

The respiratory motions in left-right (LR) and superior-inferior (SI) direction were simulated. Mapcheck XY/4D Table moving in $X$ and $Y$ direction was controlled by a computer code, and its motion patterns were edited. The image quality phantom was fixed on the top of Mapcheck XY/4D Table.

### 2.2 Motion track model and simulating curve

Referring the studies of Lujan *et al.*[8] and George *et al.*[9], with longer end-expiration than end-inspiration, the motion track model for breath is expressed by Eq.(1) in SI and AP (anterior- posterior) directions.

$$Y(t) = B_Y\ [\cos^4(\pi t/\tau) - 1/2]$$
$$X(t) = B_X\ [\cos^4(\pi t/\tau - \varphi) - 1/2] \qquad (1)$$

Supported by National Natural Science Foundation of China (Grant No. 10975187) and clinic research grant (No. LC2009B34) from the Cancer Institute

* Corresponding author. *E-mail address:* jianrong_dai@yahoo.com; wangshi@mail.tsinghua.edu.cn

Received: 2010-07-15

where, $B_X$ and $B_Y$ are the motion range in $X$ (AP) and $Y$ (SI), respectively, $\tau$ is the motion period, and $\varphi$ is the initial phase difference in $X$ and $Y$ direction to depict respiration hysteresis phenomenon.

Three motion situations were considered, referring the data of Hiroki Shirato *et al.*[10]. In the SI($Y$) direction respiratory motion, the ranges for periods of 2, 4 and 6 s were 0.75, 1.5 and 3.0 cm, respectively, but the range at the 2-s period was 2.0 cm, instead of 3.0 cm, because of the hardware limitation; while in the AP($X$) direction respiratory motion, the ranges for periods of 2, 4 and 6 s were 0.25, 0.5, and 1.0 cm, respectively.

The combined influence of SI and AP directions were measured at 4-s period with a 1.5-cm range in SI direction, and a 0.5-cm range in AP direction. To investigate the influence of hysteresis phenomenon, we set the initial phase difference in SI and AP direction to 0, π/8 and π/4. The trajectories are shown in Fig.1.

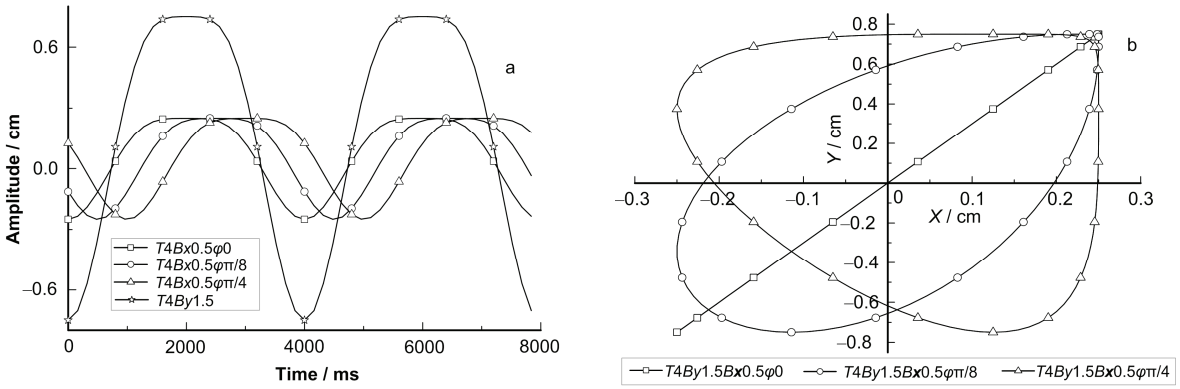


**Fig.1** Motion curves (a) and trajectories (b) for combined motion in $X$ and $Y$ direction at $T$ period. $B_X$ and $B_Y$, amplitude; and $\varphi$ initial phase difference.

We simulated 21motion states, including 9 each in AP and SI directions, and 3 for combined motion. The Mapcheck XY/4D Table can simulate the motions in just the SI or LR directions. Because the motion amplitude is larger in AP direction than in LR direction, and the cone beam CT imaging is transversely symmetrical, we used LR motion instead of AP motion.

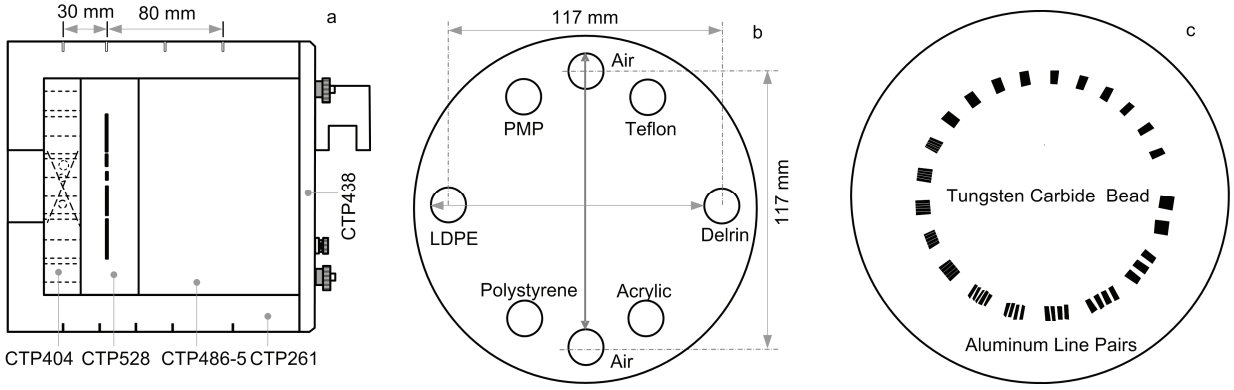


**Fig. 2** Structural diagrams of CATPHAN503 (a), CTP404 (b) and CTP528 modules (c).

### 2.3 Image quality evaluation phantom

The CatPhan503 was used to assess the image quality, and was composed of five modules (CTP404, CTP528, CTP486-5, CTP261 and CTP438), as shown in Fig.2(a). The CTP404 module of $\Phi$15 cm×25 mm was inserted with eight $\Phi$12.3 mm iterms of acrylic, two air bubbles, polystyrene, LDPE, PMP, Teflon, and Delrin (Fig.2b). The CTP528 of $\Phi$15 cm×40 mm includes 21 aluminum line pairs of 2-mm thickness, and 2 tungsten carbide beads with 0.28-mm diameter (Fig.2c). The CTP486-5 of $\Phi$15 cm ×110 mm was cast by a uniform material.

### 2.4 Image acquisition

After leveling, the Mapcheck XY/4D Table on the couch was initialized and held in "HOME" position, and the CatPhan503 was aligned with lasers. The CBCT images in static and 21 motion states were acquired on an Elekta Synergy machine (120 kV 40 mA/frame), at exposure time of 40 ms/frame, with F0 and S20 cassettes, and reconstructed in high resolution with about 650 frames.

### 2.5 Evaluation of cone beam CT images

Referring to the 3D image system QA procedure of Synergy, we used low contrast visibility, geometric accuracy, spatial resolution (line pair and MTF) and uniformity of CT values as the index to evaluate images in static and motion states.

#### 2.5.1 Low contrast visibility

The mean pixel and *SD* (standard deviation) of polystyrene and LDPE inserts in CTP404 were measured with the XVI code, and the low contrast visibility was calculated by

$$\text{Low contrast visibility} = [5.5(SD_{\text{polystyrene}} + SD_{\text{LDPE}})]/[2(\text{mean}_{\text{polystyrene}} + \text{mean}_{\text{LDPE}})] \quad (2)$$

#### 2.5.2 Geometric accuracy

For CTP404 (Fig.2b), the vertical geometric accuracy was derived by measuring center-to-center distance of the two air bubbles, and horizontal geometric accuracy by center-to-center distance of the Delrin to the LDPE. The sagittal geometric accuracy was measured by distance between Markers 1 and 4 in Fig.2(a).

#### 2.5.3 Spatial resolution

The spatial resolution was obtained by finding the CTP528 in transections and recording the highest line pair number which could be resolved, by measuring the modulation transfer function (MTF) of 50%, 10% and 0% in bead point source transection with "resolution test", the software of Philips Brilliance CT Big Bore Oncology.

#### 2.5.4 Uniformity of CT values

The mean pixel of the image center and other three random parts of the CTP486-5 images which display only the "inner circle" were recorded, and the uniformity of CT values was calculated by

$$\text{Uniformity of CT values} = [(\text{mean}_{\text{high}} - \text{mean}_{\text{low}})/\text{mean}_{\text{high}}] \times 100 \quad (3)$$

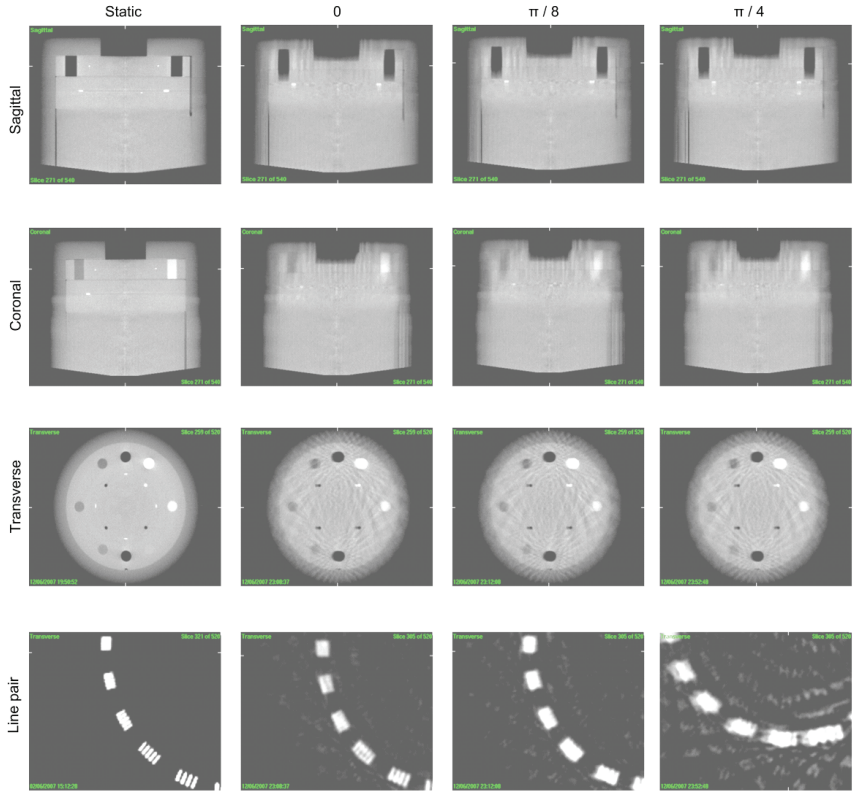


**Fig.3** CBCT images in static and motion states of 0.5-cm steps in *X* direction and 1.5-cm steps in *Y* direction at 4-s period and initial phase difference of 0, π/8 and π/4.

## 3 Results

### 3.1 Visual evaluation of image quality

Figure 3 shows the acquired CBCT images. The motion images were blurred in comparison with the static images of the moving direction. The inserts of circular cross section were blurred into oval, and the phantom was not clearly outlined, with artifacts resulted from different densities. The motion image became more blurred with increasing the phase difference from 0 to π/4.

### 3.2 Low contrast visibility

From the low contrast visibility of the images in static and motion states (Fig.4), a higher mean value could be obtained when the amplitude increased less in *X* direction motion than in *Y* direction motion. The mean value for motion in *X* direction increased with the amplitude till almost 9 times of the mean value in static, but it changed little with amplitude for motion in *Y* direction. The slope changes represents influence of the motion period, but a slope changed little in both *X* and in *Y* directions, so the period of motion in *X* and *Y* directions does not have an obvious influence on low contrast visibility. However, when another module passed the measured transection with motion amplitude increasing up to 3 cm, the image data changed dramatically to even an negative value (–101.34). The combined motion gave a similar value with the same amplitude motion in *X* direction, but it changed little with the initial phase difference.

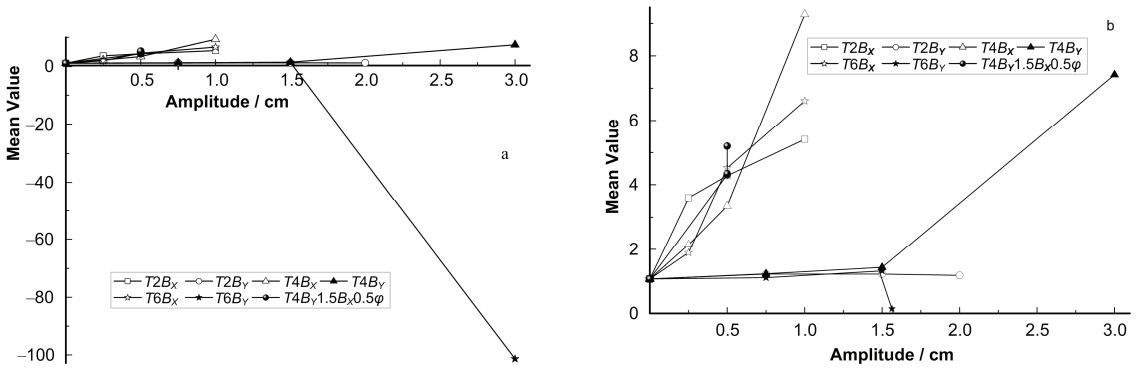


**Fig.4** Low contrast visibility of the images in static and motion states. In the right part, the negative value is ignored.

**Table 1** Geometric accuracy in vertical, horizontal, and sagittal directions.

| Test conditions | Vertical/ mm | Error / mm | Horizontal/ mm | Error / mm | Sagittal/ mm | Error / mm |
|---|---|---|---|---|---|---|
| Static | 116.70 | — | 116.60 | — | 110.10 | — |
| $T2B_X0.25$ | 116.50 | –0.2 | 117.20 | 0.6 | 109.90 | –0.2 |
| $T2B_X0.5$ | 116.60 | –0.1 | 116.80 | 0.2 | 109.90 | –0.2 |
| $T2B_X1.0$ | 116.50 | –0.2 | 116.40 | –0.2 | 110.10 | 0 |
| $T2B_Y0.75$ | 116.80 | 0.1 | 116.80 | 0.2 | 110.10 | 0 |
| $T2B_Y1.5$ | 116.70 | 0 | 116.70 | 0.1 | 110.00 | –0.1 |
| $T2B_Y2.0$ | 116.60 | –0.1 | 116.90 | 0.3 | 110.10 | 0 |
| $T4B_X0.25$ | 116.70 | 0 | 116.70 | 0.1 | 110.00 | –0.1 |
| $T4B_X0.5$ | 116.70 | 0 | 116.80 | 0.2 | 110.10 | 0 |
| $T4B_X1.0$ | 117.00 | 0.3 | 116.40 | –0.2 | 110.40 | 0.3 |
| $T4B_Y0.75$ | 116.90 | 0.2 | 117.20 | 0.6 | 110.20 | 0.1 |
| $T4B_Y1.5$ | 116.90 | 0.2 | 117.20 | 0.6 | 110.10 | 0 |
| $T4B_Y3.0$ | 117.00 | 0.3 | 117.00 | 0.4 | 110.20 | 0.1 |
| $T6B_X0.25$ | 116.70 | 0 | 117.00 | 0.4 | 110.10 | 0 |
| $T6B_X0.5$ | 116.70 | 0 | 117.00 | 0.4 | 110.10 | 0 |
| $T6B_X1.0$ | 116.70 | 0 | 117.10 | 0.5 | 110.00 | –0.1 |
| $T6B_Y0.75$ | 116.70 | 0 | 116.70 | 0.1 | 110.00 | –0.1 |
| $T6B_Y1.5$ | 116.90 | 0.2 | 117.00 | 0.4 | 109.90 | –0.2 |
| $T6B_Y3.0$ | 117.00 | 0.3 | 116.80 | 0.2 | 110.00 | –0.1 |
| $T4B_Y1.5B_X0.5\varphi0$ | 116.90 | 0.2 | 117.00 | 0.4 | 110.00 | –0.1 |
| $T4B_Y1.5B_X0.5\varphi\pi/8$ | 116.90 | 0.2 | 116.90 | 0.3 | 110.00 | –0.1 |
| $T4B_Y1.5B_X0.5\varphi\pi/4$ | 116.80 | 0.1 | 117.00 | 0.4 | 110.10 | 0 |

### 3.3 Geometric accuracy

Table 1 shows that the geometric accuracy of images in vertical, horizontal and sagittal directions for 21 motion states within 0.6 mm(~0.51%).

### 3.4 Spatial resolution

Figure 5 shows spatial resolution of the image in static and motion states. From Fig.5(a), the resolved aluminum line pairs were 7 for static, 6 for *X* direction motion, 7 for *Y* direction motion (but 6 for 3-cm amplitude) and 7 for combined motion. The spatial resolution changed more with *X* direction motion than with *Y* direction motion, but it changed little with amplitude and period variation in all motions. Also, the combined motion affected the resolution the same way as amplitude in *Y* direction, and the resolution increased with initial phase difference. From Figs.5 (b–d), motion in *X* direction did not have an obvious effect on resolution of the MTF line pairs, which changed little with amplitude and period variation, whereas it could be greatly affected by motions in *Y* direction and combined motions, changing markedly with amplitude, period and initial phase difference.

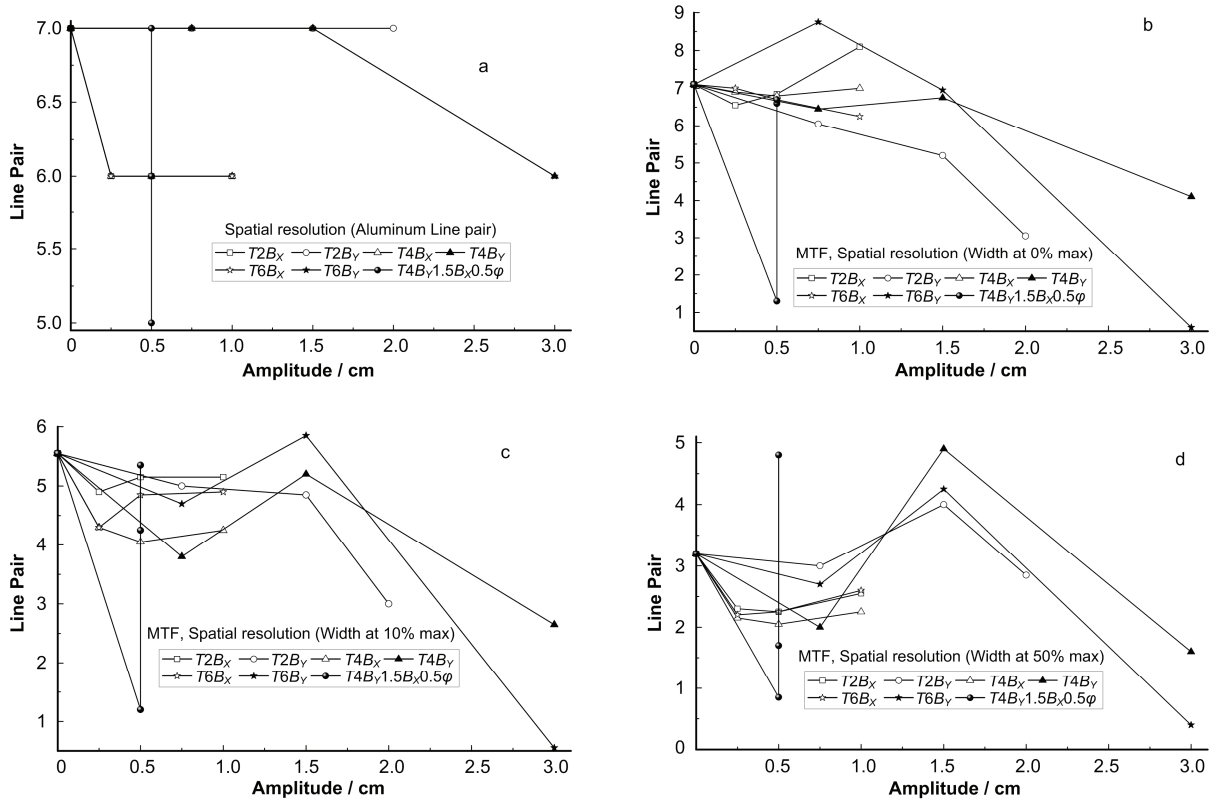


**Fig. 5** Spatial resolution with line pair and MTF.

### 3.5 Uniformity of CT values

From Fig. 6, the CT image uniformity is of almost the same tendency as the low contrast visibility. It changed more rapidly with motion in *X* direction than in *Y* direction, and increased with amplitude, but changed little with period variation for motion in *X* and *Y* directions. The uniformity for combined motion was close to the mean of motion in *X* and *Y* directions under the same amplitude, but it increased with initial phase difference variation.

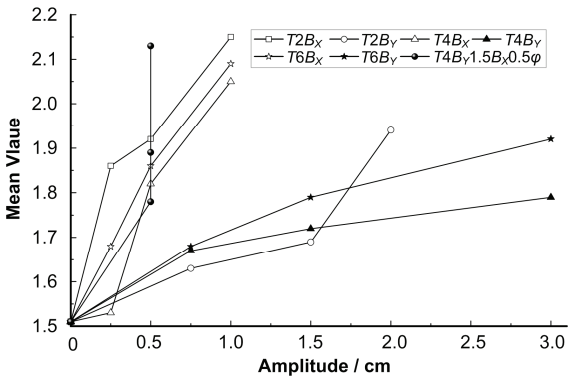


**Fig.6** CT image uniformity.

## 4 Discussion

Separate and combined motions in *X* and *Y* directions were investigated. Except for the sagittal geometric accuracy, all the data were measured in transverse section. For the amplitude variation does not cause an evident change for CT value of the object in the measurement plane, the motion in *X* direction affects more than motion in *Y* direction does, in low contrast visibility, line pairs and uniformity of the images. Otherwise, the motion in *Y* direction affects more than motion in *X* direction does in MTF.

The low contrast visibility increases greatly with the amplitude in *X* direction motion, but changes little with period variation in *X* and *Y* direction motions, and with amplitude variation for *Y* direction motion. For another module of different intensity, such as CTP528, passing the measurement transection with increasing amplitude, the low contrast visibility value changes dramatically, even to an negative value. The low contrast visibility is affected by the combined motion in the same way as amplitude motion in *X* direction, but it changes little with initial phase difference.

With fixed distance between the inserts of distinct difference in density from the surrounding, the image geometries in all motion images are accurate. Because the aluminum line pairs in CTP528 are circularly arranged with the aluminum line pairs plane being parallel to *X* direction and vertical to *Y* direction, resolution of the aluminum line pairs is greatly affected by the motion in *X* direction, but it changes little with amplitude and period variation in all motions. The line pair resolution is affected by combined motion in a similar way to the *Y* direction motion in the same amplitude, increasing with the initial phase difference. The changes in line pair value of MTF in *X* direction are different from those in *Y* direction. This is because of the small bead point source, just like the interference from insert of different intensities in low contrast visibility. The small bead point moves in the measurement plane for *X* direction motion, but it moves vertically to the measurement plane for *Y* direction motion. So motion in *X* direction affects MTF less than motion in *Y* direction, and no obvious changes can be observed by varying the amplitude and motion period. And the MTF changes markedly in *Y* direction motion by varying the amplitude and motion period, and so does the combined motion of different initial phases.

Because the *X* direction motion changes the shape of Catphan 503 in measured transection, uniformity of CT values increases greatly with the amplitude but little with motion period; while it is less affected by the *Y* direction motion. Effect of the combined motion on uniformity of CT values is about an average of the effects of the *X* and *Y* direction motion in the same amplitude, and the uniformity increases greatly with the initial phase.

Ju-Young Song *et al.*[7] simulated 1D respiratory motion, and assessed the image quality with the CT number variations along the center line of coronal images. Obviously, they made these simplifications: respiration motion was reduced from 3D to 1D; image quality in the whole image volume was evaluated with single index instead of multiple indexes. Therefore our study is much comprehensive.

## 5 Conclusions

The phantom and the evaluation method used in this study were designed for static CBCT images, and there are some limitations with the results here. But quality of motion CBCT images could be resolved by the following improvements: (1) the functional inserts, such as polystyrene and LDPE, should be large enough, and be changeable according to experimental needs; and (2) the arrangement, thickness and gaps of the line pairs should be optimized.

## References

1 Létourneau D, Martinez A A, Lockman D, *et al*. Int J Radiat Oncol Biol Phys, 2005, **62:** 1239–1246.

2 White E A, Cho J, Vallis K A, *et al*. Int J Radiat Oncol Biol Phys, 2007, **68:** 547–554.

3 Borst G R, Sonke J J, Betgen A, *et al*. Int J Radiat Oncol Biol Phys, 2007, **68:** 555–561.

4 Oelfke U, Tücking T, Nill S, *et al*. Med Dosim, 2006, **31:** 62–70.

5 Chen J, Morin O, Aubin M, *et al*. Br J Radiol, 2006, **79S1:** 87–98.

6 Burridge N, Amer A, Marchant T, *et al*. Int J Radiat Oncol

Biol Phys, 2006, **66:** 892–897.

7 Song J Y, Nam T K, Ahn S J, *et al.* Med Dosim, 2009, **34:** 117–125.

8 Lujan A E, Larsen E W, Balter J M, *et al.* Med Phys, 1999, **26:** 715–720.

9 George R, Vedam S S, Chung T D, *et al*. Med Phys, 2005, **32:** 2850–2861.

10 Shirato H, Seppenwoolde Y, Kitamura K, *et al*. Semin Radiat Oncol, 2004, **14:** 10–18.